THE EFFECT OF HEAT TREATMENT UNDER VARIOUS CONDITIONS ON MICROSTRUCTURE OF SINTERED (Nd,Pr,Dy)-Fe-B MAGNETS

Yurij S. KOSHKID'KO[a], Kateřina SKOTNICOVÁ[a], Miroslav KURSA[a], Tomáš ČEGAN[a], Gennadij S. BURKHANOV[b], Natalia B. KOLCHUGINA[b], A. A. LUKIN[c], A. G. Dormidontov[c], V. V. SITNOV[c]

[a]*VSB-Technical University of Ostrava, Ostrava, Czech Republic, EU, Katerina.Skotnicova@vsb.cz*
[b]*Baikov Institute of Metallurgy and Materials Science, Russian Academy of Sciences, , Moscow, Russian Federation, natalik@imet.ac.ru*
[c]*"JSC SPETSMAGNIT", Moscow, Russian Federation, lukinikul@rambler.ru*

Abstract

The use powder mixtures, which consists of strip-casting (Nd,Pr)-Fe-B alloy and DyH_2 hydride, allows the high-coercivity magnets to be prepared. The stability of the reached high magnetic characteristics in the course of both low- and high-temperature heat treatments was shown to be related to the evolution of grain structure of the magnets. The microstructure and chemical composition of the permanent magnets were studied by electron microscopy (SEM/EDX) using a Quanta 450 FEG microscope. Electron microscopic studies of their microstructure demonstrated annealing-induced changes in the thickness and continuity of $(Nd,Pr,Dy)_2Fe_{14}B$-phase grain boundaries and the shape of triple junctions of the grains. Electron microprobe analysis of triple junctions revealed the presence of various (Nd,Pr,Dy)-O oxides such as (Nd,Pr,Dy)O, $(Nd,Pr,Dy)_2O_3$ and $(Nd,Pr,Dy)O_2$. The studies performed allow us to conclude the effect of heat treatment of the principal structural and magnetic characteristics of permanent magnets.

Keywords: Permanent magnets, strip casting, grain boundaries.

1. INTRODUCTION

Sintered Nd-Fe-B magnets find wide applications for technology owing to the high maximum energy product $(BH)_{max}$, residual inductance B_r and magnetization coercive force ${}_jH_c$. Nd-Fe-B permanent magnets are used in many fields of industry. One of problems of preparation of permanent magnets based on the $Nd_2Fe_{14}B$ compound is related to the decrease in the content of non-magnetic phases via the optimization of the rare-earth metals contents. The strip-casting technology allows one to decrease the content of rare-earth metals in Nd-Fe-B permanent magnets and optimize their phase composition [1-2].

Another problem is to increase the thermal stability and coercive force of permanent magnets. The addition of heavy rare earths as Dy or Tb is effective to enhance coercivity and consequent thermal stability of the Nd-Fe-B magnets, because they increase the magnetic anisotropy field of the Nd-Fe-B compound, but this method simultaneously results in considerable degradation of the remanence of magnets [1-4]. Recently, techniques for enhancement of coercivity of sintered Nd-Fe-B magnets by diffusing a continuous layer of Dy or Tb onto the surface of the $Nd_2Fe_{14}B$ matrix grains without obvious reduction of the remanence have been developed by different researchers [1-8], but the detailed mechanism for the improving coercivity is unclear.

The experiments with Dy and Tb additions are carried out to achieve the optimum microstructure, which involves confining the Dy distribution to the grain boundary regions. If the Dy can be confined in grain boundary regions, then:

1) It should be possible to increase locally the coercivity and hence reduce the probability of reverse domains forming at the grain boundaries.
2) Limit the substitution of Nd by Dy in the matrix phase and thus limit the reduction of the magnetization

and hence the remanence.

3) Reduce the amount of Dy required to achieve a particular increase in the coercivity and hence reduce the overall cost of the alloy.

This paper is aimed at microstructural studies of prepared Nd-Fe-B-based magnets after heat treatment under various conditions, which were performed for understanding the phase composition of near-grain boundary regions and triple joints of grains.

2. EXPERIMENTAL

Nd-Fe-B magnets were prepared using Nd - 24, Pr - 6.5, Dy - 0.5, B - 1, Al - 0.2, Fe - 65.8 [wt.%] strip-casting alloy. The preparation procedure includes the hydrogen decrepitation of flakes in dry hydrogen (at 100 °C for 1 h) and subsequent passivation in gaseous nitrogen atmosphere. Dysprosium hydride (2 wt.%) was added after cooling of the powder to room temperature. The mixture was subjected to fine milling for 40 minutes to an average particle size of 3 μm using a vibratory mill and isopropyl alcohol medium. Powder samples were compacted in a magnetic field and sintered at t = 1070 °C (for 2 h). The sintered blanks were subjected to the following heat treatments:

- *HT-1* (optimum): 550 °C (1 h) + quenching in gaseous nitrogen (Sample No.1);
- *HT-2*: 550 °C (1 h) + quenching + 500 °C (2h) + quenching + 500 °C + cooling for 2 h to 400 °C + 400 °C (6 h) + furnace cooling (in this case, the properties are almost unchanged, although the earlier experiments performed for similar magnets demonstrates the decrease in magnetic properties jHc and Hk) (Sample No. 2);
- *HT-3*: 550 °C (1 h) + quenching + 500 °C (2h) + quenching + 500 °C + cooling for 2 h to 400 °C + 400 °C (6 h) + furnace cooling + 550 °C (1h) + quenching (properties decreases substantially (Sample No. 3).

Earlier studies showed the partial or complete recovery of properties and even their increase for high-alloyed (with Dy, Tb, Co, Ti, Mo, V, Nb) magnets.

Magnetic properties are given in **Fig. 1**. The measurements were performed at room temperature using a closed circuit of hysteresisgraph and samples 40 mm in diameter and 8 mm thick, which were subjected to HT-1, HT-2, and HT-3. The demagnetization curve for sample No. 3 showed a significant decrease in the coercive force of in comparison to the samples No. 1, 2. It is known from the literature [1-13] that the coercive force of the permanent magnet largely depends on the chemical composition and microstructure of the samples. For this reason, the complex microstructure and phase composition of samples were investigated by SEM/EDX using Quanta 450 FEG microscope.

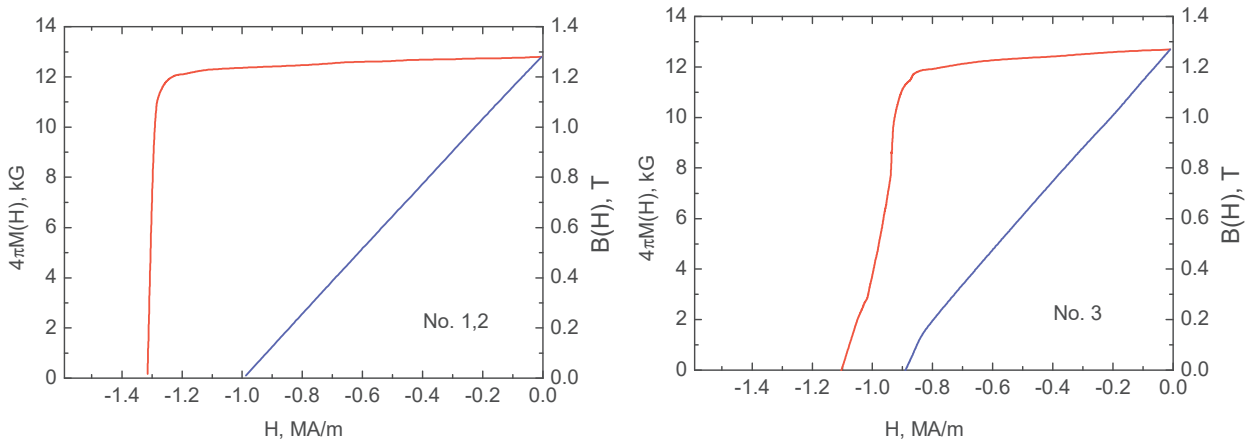

Fig.1 Demagnetization curves for samples No. 1-3.

3. RESULTS AND DISCUSSION

3.1 Chemical analysis

As is seen from **Table 1**, the contents of elements agree well with the composition of initial strip-casting charge with 2 wt.% DyH_X additions (Nd - 24, Pr - 6.5, Dy - 0.5 + 2 DyH_X , B - 1, Al - 0.2, Fe - 65.8 [wt.%]). Small differences in the chemical compositions of magnets and initial strip-casting alloy are due to the presence of small amount of oxygen (~3 %).

Based on the analysis of chemical composition and literature data [10-12], we assumed the presence of REM oxide phases in ternary junctions of samples under study. According to these literature data, ternary junctions can contain different oxide phases. These are NdO with the NaCl-type structure (space group Fm-3m) [12] (the oxygen content is 50 at.%), Nd_2O_3 with the La_2O_3-type structure (space group Pm-3m) (the oxygen content is 60 at.%) [10-11], and NdO_2 with the CaF_2-type structure (space group Fm-3m) (the oxygen content is 67 at.%) [13].

As is seen form **Table 2**, oxygen is present in ternary junctions (white areas in **Fig. 1**). In this case, as is seen from **Table 2**, the atomic percentage of elements in ternary junctions corresponds to phases with the stoichiometric compositions close to the Nd_2O_3 or NdO phases. The presence of these phases in the samples is also confirmed by the X-ray diffraction analysis data.

The stoichiometric composition of grains is close to that of the 2:14:1 phase. However, as is seen from the calculation of the Fe/R ratio, some differences take place (**Table 3**). This is related to the existence of errors of determination of the phase composition, which are due to the closeness of characteristic X-ray spectra of some elements. In particular, the excitation potential for the L_α - series of Dy is 6.494 keV, whereas for Fe, the excitation potential for Fe K_α is 6.403 keV. Therefore, we must take spectra with the lower intensity; this can give error in determining the quantitative phase composition of material. In this case for Dy, we used the Mα (1.293 keV) characteristic radiation for Dy. Another difficulty exists in determining the chemical composition for the area (since the electron beam diameter is ~ 2 μm). The aforementioned facts are the causes for the indefinite determination of the phase composition at a point. Moreover, electron beam penetrates deep into a sample and sampling area is pear-shaped of a certain diameter. This is one more cause for the differences in the phase composition of studied phases. In this case, it was impossible, in using the Quanta 450 FEG electron microscope, to determine the chemical composition of grain boundaries since the width of them is 3-4 nm [13]. However, it is known from the literature that grain boundaries are formed by R-rich phase. The investigation of grain boundaries is presented in the next section.

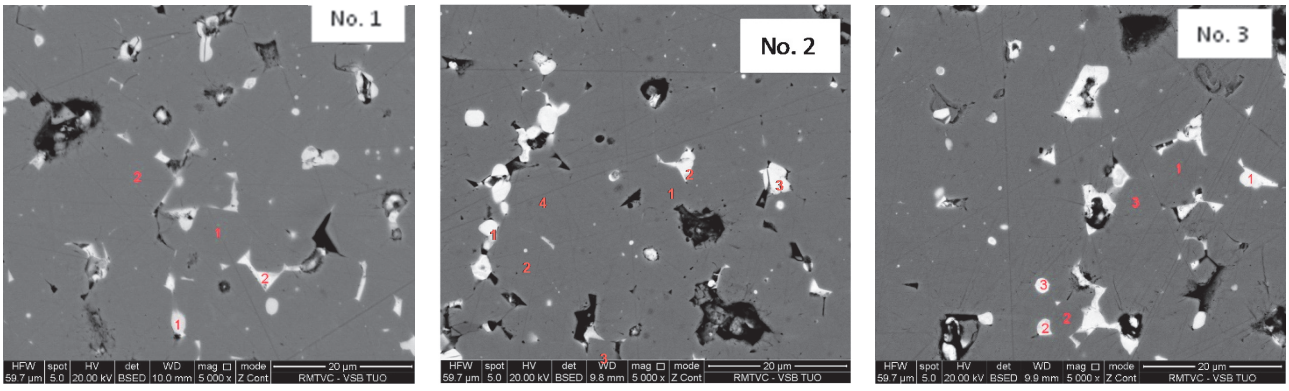

Fig. 2 SEM image of the surface of sample No. 1-3 (for **Tables 2 - 3**).

Table 1 Content of elements determined on the surface of metallographic sections of permanent magnet samples

Sample		OK	DyM	PrL	NdL	TbL	FeK	CoK
No. 1	[wt.%]	3.04	2.74	6.95	23.4	0	63.75	0.12
	[at.%]	12.16	1.08	3.16	10.39	0	73.08	0.13
No. 2	[wt.%]	3.84	2.89	6.53	22.82	0	63.82	0.11
	[at.%]	14.93	1.11	2.88	9.85	0	71.12	0.11
No. 3	[wt.%]	3.24	2.95	7.3	24.06	0	62.19	0.25
	[at.%]	12.99	1.17	3.33	10.72	0	71.53	0.27

Table 2 Chemical composition of phases in triple junctions [at.%]

Sample	Phase	OK	DyM	PrL	NdL	TbL	FeK	CoK
No. 1	Phase 1	55.50	2.47	8.53	24.85	0	8.21	0.44
	Phase 2	13.86	0.91	16.60	33.02	0	31.79	3.81
	Phase 3	28.95	1.11	8.51	22.56	0	37.98	0.89
No. 2	Phase 1	58.37	2.76	8.14	23.83	0	6.69	0.21
	Phase 2	53.56	2.76	9.15	27.08	0	7.13	0.32
	Phase 3	59.56	2.58	8.22	24.09	0.11	5.02	0.41
No. 3	Phase 1	55.23	1.81	8.79	25.83	0	8.33	0.00
	Phase 2	43.83	1.90	8.66	26.64	0	18.82	0.15
	Phase 3	46.90	3.39	9.15	27.79	0	12.78	0.00
	Phase 4	16.55	1.55	17.73	39.05	0	22.19	2.94

Table 3 Chemical composition of grains in permanent magnets [at.%]

Sample	Phase	OK	DyM	PrL	NdL	TbL	FeK	CoK	Fe/R
No. 1	Phase 1	6.95	0.8	2.86	9.63	0	79.76	0	6.00
	Phase 2	6.93	1.2	2.84	9.37	0	79.45	0.22	5.94
No. 2	Phase 1	7.19	0.9	2.93	9.45	0	79.29	0.24	5.99
	Phase 2	7.35	1.07	2.74	9.6	0	79.24	0	5.91
	Phase 3	6.87	0.53	2.74	9.87	0	80	0	6.09
	Phase 4	7.09	0.23	2.75	9.81	0	79.8	0.32	6.26
No. 3	Phase 1	6.97	0.64	2.76	9.59	0	79.84	0.2	6.16
	Phase 2	6.78	0.51	3	9.85	0	79.68	0.17	5.98
	Phase 3	7.33	0.37	2.88	9.84	0	79.42	0.16	6.08

3.2 Study of grain boundaries

SEM-images of grain boundaries in samples No.1-3 are documented in **Fig. 3**. To decrease the image blur, the scanning time was increased.

As is evident from **Fig. 3**, grain boundaries are seen clearly for samples No. 1 and 2. The structure of grain boundaries in sample No. 3 is discontinuous and in some areas, grain boundaries are almost vanishes (or invisible). In [13], the effect of annealing temperature on the state of grains boundaries and magnetic properties

of Nd-Fe-B magnets was studied. It was shown that discontinuous grain boundaries lead to a decrease in the coercive force. As mentioned above, grain boundaries are formed by a paramagnetic R-rich phase. The R-rich phase layer provides magnetic isolation of grains. This increases the resistance to demagnetization grain. Therefore, if there are more smooth grain boundaries, the coercive force of the permanent magnets is increased.

However, in our case, to conclude definitely the effect of state of grain boundaries on the coercive force, additional studies by high-resolution microscopy should be performed.

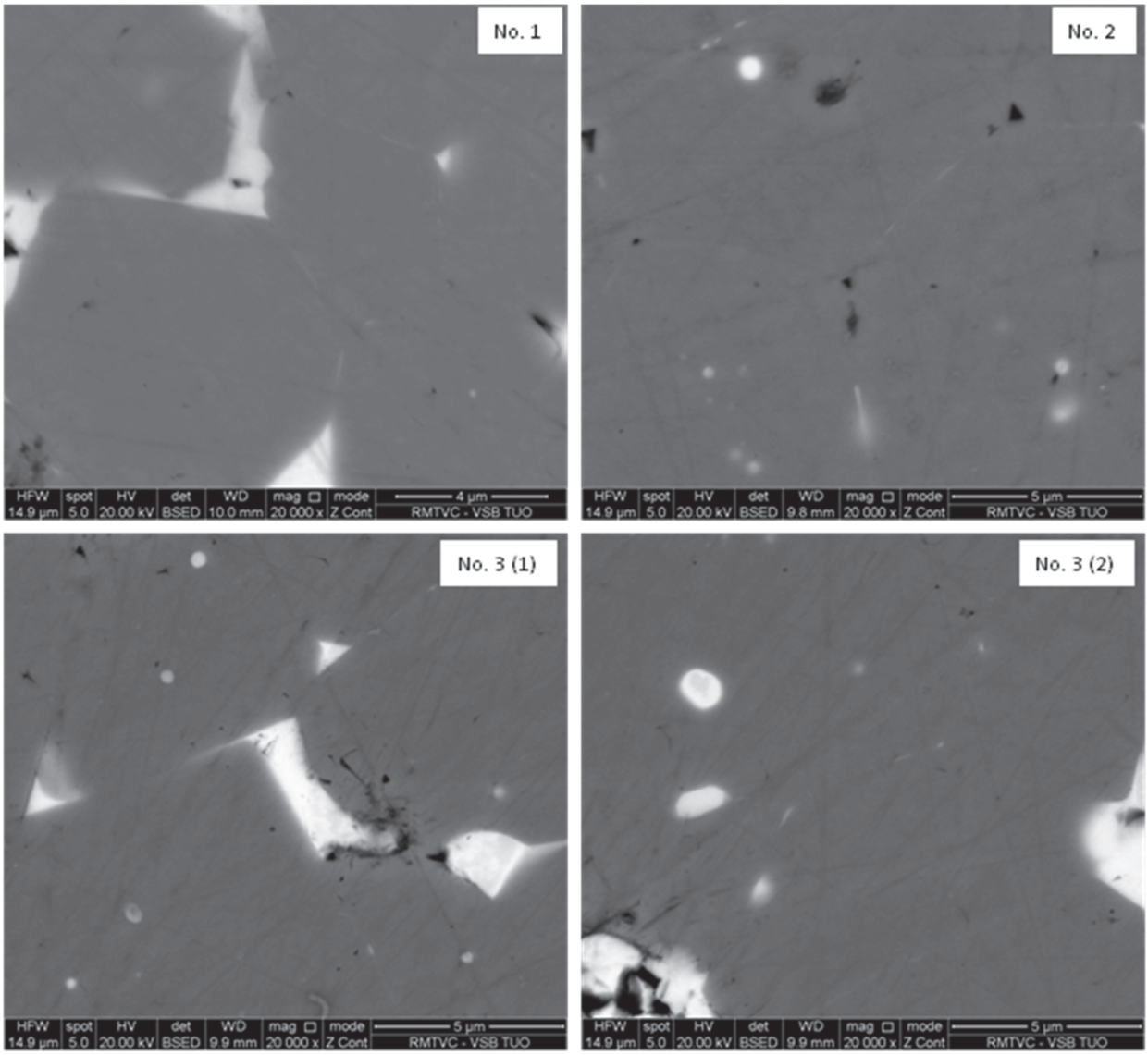

Fig. 3 SEM images of grain boundaries in samples No. 1-3.

CONCLUSION

Samples of high-coercivity (Nd,Pr)-Fe-B magnets were prepared using powder mixture containing DyH_2. The effect of heat treatment on the microstructure of permanent magnets and the chemical composition of samples was investigated using of electron microscopy. Chemical analysis of grains and triple junctions revealed no correlation with the heat treatment regimes. In this case, the state of grain boundaries should be considered the main reason of decrease in coercive force of permanent magnets.

ACKNOWLEDGEMENTS

This paper has been elaborated in the framework of the project Opportunity for young researchers, reg. no. CZ.1.07/2.3.00/30.0016, supported by Operational Program Education for Competitiveness and co-financed by the European Social Fund and the state budget of the Czech Republic and in the project No. LO1203 "Regional Materials Science and Technology Centre - Feasibility Program" funded by Ministry of Education, Youth and Sports. This study was also supported by the Branch of Chemistry and Materials Science, Russian Academy of Sciences (program no. 5).

REFERENCES

[1] KOLCHUGINA, N., LUKIN, A., BURKHANOV, G.S., SKOTNICOVÁ, K., DRULIS, H., PETROV, V. Role of terbium hydride additions in the formation of microstructure and magnetic properties of sintered Nd-Pr-Dy-Fe-B magnets. In *Metal 2012: 21th International Conference on Metallurgy and Materials.* May 23rd-25th 2012 Brno, Czech Republic. Ed. Ostrava: Tanger s.r.o., 2012, pp. 1387-1392.

[2] LUKIN, A.A., KOLCHUGINA, N.B., BURKHANOV, G.S, KLYUEVA, N.E., SKOTNICOVA, K. Role of terbium hydride additions in the formation of microstructure and magnetic properties of sintered Nd-Pr-Dy-Fe-B magnets. *Inorganic Materials: Applied Research*, 2013, Vol. 4, No. 3, pp. 256-259.

[3] LIU, W.Q., SUN, H., YI, X.F., LIU, X.C., ZHANG, D.T., YUE, M., ZHANG, J.X. Coercivity enhancement in Nd-Fe-B sintered permanent magnet by Dy nanoparticles doping. *Journal of Alloys and Compounds*, 2010, Vol. 501, pp. 67-69.

[4] YUE, M., LIU, W.Q., ZHANG, D.T., JIAN, Z.G., CAO, A.L., ZHANG, J.X. Tb nanoparticles doped Nd-Fe-B sintered permanent magnet with enhanced coercivity. *Applied Physics Letters*, 2009, Vol. 94, 092501.

[5] GAOLIN, Y., MCGUINESS, P.J., FARR, J.P.G., HARRIS I.R. Optimisation of the processing of Nd-Fe-B with dysprosium addition. *Journal of Alloys and Compounds*, 2010, Vol. 491, L20-L24.

[6] POPOV, A.G., VASILENKO, D.Yu., PUZANOVA, T.Z., SHITOV, A.V., VLASYUGA, A.V. Effect of diffusion annealing on hysteretic properties of sintered Nd-Fe-B magnets. *The Physics of Metals and Metallography*, 2011, Vol. 111, No. 5, pp. 471-478.

[7] LI, W.F., SEPEHRI-AMIN, H., OHKUBO, T., HASE, N., HONO, K. Distribution of Dy in high-coercivity (Nd,Dy)-Fe-B sintered magnet. *Acta Materialia*, 2011, Vol. 59, pp. 3061-3069.

[8] SEPEHRI-AMIN, H., UNE, Y., OHKUBO, T., HONO, K., SAGAWA, M. Microstructure of fine-grained Nd-Fe-B sintered magnets with high coercivity. *Scripta Materialia*, 2011, Vol. 65, pp. 396-399.

[9] SEPEHRI-AMIN, H., OHKUBO, T., HONO, K. Grain boundary structure and chemistry of Dy-diffusion processed Nd-Fe-B sintered magnets. *Journal of Applied Physics*, 2010, Vol. 107, 09A745.

[10] KIM, T.H., LEE, S.R. NAMKUMG, S., JANG, T.S. A study on the Nd-rich phase evolution in the Nd-Fe-B sintered magnet and its mechanism during post-sintering annealing. *Journal of Alloys and Compounds*, 2012, Vol. 537, pp. 261-268.

[11] WANG, S.C., LI, Y. In situ TEM study of Nd-rich phase in NdFeB magnet. *Journal of Magnetism and Magnetic Materials*, 2005, Vol. 285, pp. 177-182.

[12] WATANABE, N., UMEMOTO, H., ITAKURA, M., NISHIDA, M., MACHIDA K. Grain boundary structure of high coercivity Nd-Fe-B sintered magnets with Tb-metal vapor sorption. In *IOP Conf. Series: Materials Science and Engineering*, 2009, Vol. 1, 012033.

[13] VIAL, F., JOLY, F., NEVALAINEN, E., SAGAWA, M., HIRAGA, K., PARK, K.T. Improvement of coercivity of sintered NdFeB permanent magnets by heat treatment. *Journal of Magnetism and Magnetic Materials*, 2002, Vol. 242-245, pp. 1329-1334